Journal of Materials Chemistry C

PAPER

View Article Online
View Journal | View Issue

Cite this: J. Mater. Chem. C, 2014, 2, 9637

Upconversion luminescence nanoparticles-based lateral flow immunochromatographic assay for cephalexin detection†

Chunyan Liu,[a] Wei Ma,[b] Zhenyu Gao,[c] Jiayi Huang,[a] Yi Hou,[a] Chuanlai Xu,[b] Wensheng Yang[c] and Mingyuan Gao*[a]

Received 11th September 2014
Accepted 29th September 2014

DOI: 10.1039/c4tc02034k

www.rsc.org/MaterialsC

Because of the near infrared excitation, upconversion luminescence (UCL) rare-earth nanoparticles are very suitable for biological applications in terms of low background interference. $NaGdF_4$:Yb,Er nanoparticles were firstly synthesized through a replacement reaction at high temperature. To improve the upconversion luminescence efficiency, core–shell $NaGdF_4$:Yb,Er@$NaGdF_4$ nanoparticles were then prepared by a seed-mediated method. The core–shell architecture significantly improved the upconversion luminescence and more effectively retained the luminescence during the following phase transfer process by ligand exchange. Upon further coupling with anti-cephalexin monoclonal antibody *via* "click" reaction, the resultant upconversion luminescence probe was obtained and used in a lateral flow immunochromatographic assay (LFIA) to detect the antibiotic residue of cephalexin. The results were compared with those achieved by a nanoprobe assay based on gold nanoparticles. More quantitative results were extracted by luminescent intensity analysis. Under optimized conditions, the detection limit of UCL nanoparticles-based LFIA was considerably comparable with gold nanoparticles-based LFIA.

Introduction

The lateral flow immunochromatographic assay (LFIA), also known as lateral flow test, has been widely used for environmental monitoring,[1] food safety monitoring,[2] and medical diagnosis,[3] in particular home testing[4] and point of care testing,[5] during the past twenty years. The technique of LFIA incorporates the immune recognition reaction and capillary action of thin layer chromatography. Colored particles such as colloidal gold have been most widely adopted in LFIA to be antibody labels. Because of the excellent chemical stability and vivid red color caused by localized surface plasmon resonance of Au nanoparticles, colloidal gold nanoparticles-based LFIA can be used for the qualitative or semi-quantitative detection of various target analytes in solutions through colorimetric detection either by naked eyes or with the aid of optical density analysis. Other particles including selenium,[6] carbon,[7] and latex[8] were also applied in LFIA.

Moreover, developing new labeling materials provides additional means in addition to optical density, such as the detection based on magnetic or fluorescent signals, for improving the detection sensitivity.[9–11] For example, luminescent materials including organic dyes and inorganic semiconductor quantum dots (QDs) have emerged to be suitable optical labels in LFIA.[12,13] The high sensitivity of fluorescence detection provides them enormous potential in biological analysis. However, intrinsic limitations are not overcome, such as the photobleaching of the probe and background signals of residues beyond the analyte.

Upconversion luminescence (UCL) rare-earth nanoparticles as novel and alternative luminescent materials have attracted increasing interest in biological labeling and detection.[14,15] Upconversion luminescence is a nonlinear optical process *via* a two-photon or multi-photon absorption mechanism, which can convert long-wavelength near-infrared (NIR) radiation into short-wavelength visible light. UCL materials have attractive luminescence characteristics, such as large effective Stokes shifts, sharp emissions, long fluorescence lifetimes, and high resistance to photobleaching.[14] Because upconversion luminescence is typically absent or low for most of the materials in contrast to fluorescence, the detection based on UCL particles is characterized by high signal-to-noise ratios, which makes the UCL particles potentially useful to be labels for LFIA.

Herein, we report a sensitive lateral flow immunochromatographic assay based on UCL nanoparticles. In fact, antibiotic

[a]Institute of Chemistry, Chinese Academy of Sciences, Bei Yi Jie 2, Zhong Guan Cun, Beijing 100190, China. E-mail: gaomy@iccas.ac.cn; Fax: +86 10 8261 3214
[b]School of Food Science and Technology, Jiangnan University, Lihu Road 1800, Wuxi, Jiangsu Province, 214122, China
[c]College of Chemistry, Jilin University, Changchun 130012, China

† Electronic supplementary information (ESI) available: Shows the chemical stability and the optical stability of the conjugate of UCL particles with mAb. See DOI: 10.1039/c4tc02034k

abuse has become a serious worldwide issue due to the overuse in aquaculture and livestock. In consequence, the antibiotic residues left in food give rise to adverse effects on human health, such as allergic reactions, promoting the drug resistance of pathogenic bacteria that may transfer antibiotic resistance genes to human pathogens.[16,17] Cephalexin (CEX) is a β-lactam antibiotic that is widely used in veterinary medicine to treat mastitis and other infectious diseases in dairy cows. The residues in milk or other edible animal tissues will be harmful to human health.[18] Therefore, CEX is chosen to be a model antibiotic in the current study for antibiotic detection through UCL nanoparticles-based LFIA.

Following on from our previous investigations on the preparation and *in vivo* application of UCL $NaGdF_4$:Yb,Er nanoparticles,[19,20] the core–shell $NaGdF_4$:Yb,Er@$NaGdF_4$ nanoparticles were synthesized and covalently conjugated with anti-cephalexin monoclonal antibody. The conjugate was employed in the LFIA analysis of CEX, and the detection limit achieved was compared with that obtained in an assay based on colloidal gold particles.

Materials and methods

Reagents and materials

The following materials were purchased from Sigma-Aldrich: $GdCl_3 \cdot 6H_2O$ (450855), $YbCl_3 \cdot 6H_2O$ (337927), $ErCl_3 \cdot 6H_2O$ (259256), oleic Acid (OA, 364525), 1-octadecene (ODE, O806), ammonium fluoride (NH_4F, 216011), tris(2-carboxyethyl)phosphine hydrochloride (TCEP, C4706), polyvinylpyrrolidone (PVP, $M_w \sim 29\,000$, 9003398), 1-ethyl-3-(3-dimethylaminopropyl) carbodiimide (EDC, 161462), and *N*-hydroxysulfosuccinimide sodium salt (sulfo-NHS, 56485). A bifunctional ligand, PEG2000, bearing a maleimide group at one end and a diphosphate group at the other end (mal-PEG-dp) was a customized product provided by Beijing Oneder Hightech Co. Ltd. Bovine serum albumin (BSA, M_w 67 000 kD, Amresco 0332) and polyoxyethylene lauryl ether (Brij35, 9002920) were purchased from Biodee Biotechnology Beijing, Co., Ltd. Polyoxyethylene sorbitan monolaurate (Tween-20), sucrose, disuccinimidyl suberate (DSS), and other analytical grade chemicals such as K_2CO_3, ethanol, cyclohexane, and tetrahydrofuran (THF) were purchased from Sinopharm Chemical Reagent Beijing, Co., Ltd. CEX was purchased from National Research Center for Certified Reference Materials. Goat anti-mouse IgG was bought from Solarbio Science & Technology Co., Ltd. Keyhole limpet hemocyanin (KLH) and ovalbumin (OVA) were purchased from BoAo Co., Ltd. (Shanghai, China). The nitrocellulose membrane (Sartorius CN 140), glass fiber (Ahlstrom 8964 and GF-06) and absorbent paper were purchased from Jiening Biotech Shanghai, Co., Ltd.

Preparation of $NaGdF_4$:Yb,Er@$NaGdF_4$ nanoparticles

The Yb/Er-doped $NaGdF_4$ nanoparticles were prepared according to our previous report with some modifications.[20] In a typical synthesis, $GdCl_3 \cdot 6H_2O$ (0.80 mmol), $YbCl_3 \cdot 6H_2O$ (0.18 mmol), and $ErCl_3 \cdot 6H_2O$ (0.02 mmol) were mixed with 14 mL OA and 16 mL ODE in a 100 mL flask. After heating to 150 °C to form a homogeneous solution under nitrogen protection, the solution was cooled down to 50 °C and 10 mL of a methanol solution containing NaOH (2.5 mmol) and NH_4F (3.6 mmol) was added dropwise. The reaction system was then stirred at this temperature for 30 min. Subsequently, methanol in the system was removed under vacuum at 100 °C, and the formed reaction mixture was heated to 300 °C under atmospheric pressure for 1 h. The resultant nanoparticles were precipitated by ethanol, collected by centrifugation, washed with ethanol for three cycles, and finally redispersed in THF.

The subsequent deposition of the $NaGdF_4$ shell followed a similar process for the preparation of $NaGdF_4$:Yb,Er core particles. Briefly, 1 mmol $GdCl_3 \cdot 6H_2O$ was added to a 100 mL three-neck round-bottom flask containing 4 mL OA and 15 mL ODE; the mixture was heated to 150 °C under nitrogen protection to form a homogeneous solution, and then cooled to 80 °C. 0.33 mmol $NaGdF_4$:Yb,Er nanoparticles in 5 mL THF was then added. After the removal of THF, 10 mL of a methanol solution containing NaOH (2.5 mmol) and NH_4F (4 mmol) was added, and the mixture was stirred at 50 °C for 30 min. Then, methanol was removed, and the solution was heated to 300 °C under a protective N_2 atmosphere. The reaction mixture was maintained at this temperature for 60 min under magnetic stirring, and then cooled down to room temperature. The obtained core–shell nanoparticles were precipitated by ethanol, collected by centrifugation, washed with ethanol for three cycles, and finally redispersed in THF for further experiments.

Preparation of anti-CEX monoclonal antibody

The CEX immunogen, coating antigen, and anti-CEX monoclonal antibody (mAb) were prepared according to the previous literature.[18] In brief, CEX immunogen was prepared by conjugating CEX with KLH through DSS. The immunogen of CEX–KLH mixed with Freund's complete adjuvant was used to immunize BALB/c mice. Standard cell fusion techniques were used for generating mAb. CEX–BSA as coating antigen was synthesized through the (EDC/sulfo-NHS)-mediated amidation reaction between CEX and BSA.

Preparation of water-soluble nanoparticles and nanoparticles–mAb conjugate

The water-soluble nanoparticles were prepared through a ligand exchange reaction according to our previous report.[19] Approximately 10 mg of the purified nanoparticles and 100 mg of mal-PEG-dp were dissolved in 5 mL THF, and the mixture was allowed to react overnight at 40 °C. After ligand exchange, PEGylated particles were precipitated and washed with cyclohexane, and finally dried under vacuum at room temperature. The obtained nanoparticles were dispersed in water after removing the free ligand by ultrafiltration using a 100 kDa filter (Millipore) at 6000*g*.

The conjugates of $NaGdF_4$:Yb,Er@$NaGdF_4$ nanoparticles and anti-CEX mAb were prepared by the "click" reaction. Typically, anti-CEX mAb (1 mg mL^{-1}) was dispersed in 10× PBS buffer, and then subjected to mild reduction by TCEP to convert the disulfide groups in the Fc fragments to thiols. After purification using 30 K MWCO centrifugal devices, the partially

reduced antibody was mixed with (mal-PEG-dp)-coated $NaGdF_4$:Yb,Er@$NaGdF_4$ particles in tris-buffered saline (TBS, pH 7.04) at a molar ratio of 4 : 1 (mAb : nanoparticle). The resultant conjugate was transferred into 1× PBS buffer, and stored at 4 °C for further use.

The colloidal gold labeled mAb was prepared according to a previous report.[17] The solution of gold nanoparticles was adjusted to pH 8.2 with 0.1 M K_2CO_3, and then mAb solution was added drop by drop. After shaking for 2 h at room temperature, 10% BSA was added as blocking solution to reduce nonspecific binding. Finally, the solution was centrifuged at 10 000*g* to remove the unbound antibody and blocking reagent. The obtained conjugate was resuspended in PBS solution containing 10% (w/v) sucrose, 0.01% BSA, and 0.05% Tween-20.

UCL nanoparticles-based LFIA

The principle and structure of the UCL nanoparticles-based LFIA are shown in Scheme 1. The LFIA strip consists of five components including sample pad, conjugate pad, nitrocellulose (NC) membrane, absorbent pad, and backing card. The sample pad is used to apply sample solution, and the conjugate pad is used to load the particle-labeled antibody. The absorbent pad serves as the liquid sink, and the backing card is used for supporting all of the components. The NC membrane acts as the chromatography matrix. A band of goat anti-mouse IgG and a band of coating antigen (CEX–BSA) were drawn on the NC membrane as control line (C line) and test line (T line), respectively. The sample pad was pre-treated with 1× PBS buffer containing 2% (w/v) Brij-35, and the conjugate pad was pre-treated with PBS buffer containing 0.1% (w/v) BSA, 0.05% (w/v) Tween 20, and 10% (w/v) sucrose. Then, the as-prepared particle–antibody conjugate solution incubated with 2% PVP for 30 min was spotted onto the conjugate pad. After the aforementioned LFIA components dried, they were assembled with overlaps between the sample pad and conjugate pad and between the conjugate pad and the NC membrane with a thickness of 2 mm to ensure proper solution migration through the strip during the detection procedure.

Competitive assays were run by applying 100 μL of CEX in 1× PBS solution with a series of concentrations to the sample pad in a controlled environment with a relative humidity of 40–50%. After approximately 20 min, the luminescence of the testing strip was recorded under a constant 980 nm excitation by a CW laser. Then, the luminescence intensity was obtained by integrating luminescence signals of both T and C lines.

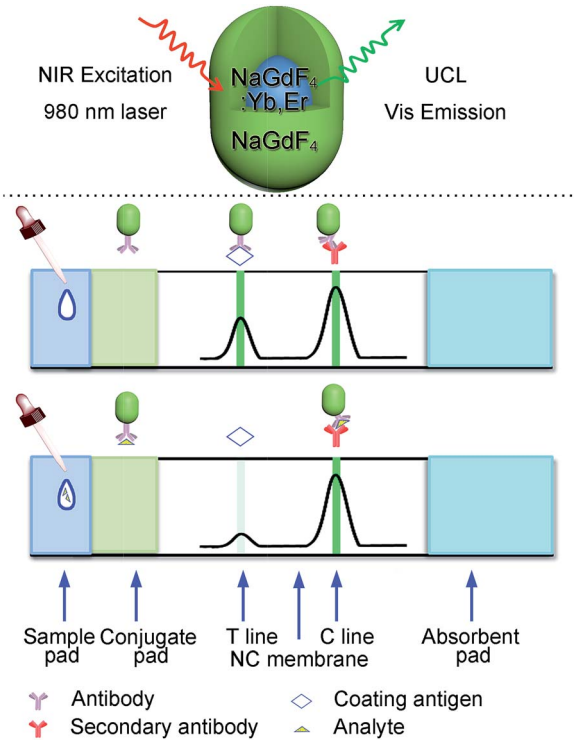

Scheme 1 Schematic drawing for the core–shell structured upconversion luminescence nanoparticles (upper panel), and the competitive LFIA principle based on UCL nanoparticles (lower panel).

Characterization

Transmission Electron Microscopy (TEM) measurements were carried out with a JEM-100CXII microscope operating at an accelerating voltage of 100 kV for characterizing the UCL nanoparticles. The concentration of the rare earth elements in the nanoparticles was determined by inductively coupled plasma atomic emission spectrometer (ICP-AES) produced by Jiangsu Skyray instrument Co., Ltd after the particles were dissolved in concentrated nitric acid. The UCL spectra were recorded on a Cary Eclipse fluorescence spectrophotometer equipped with a 980 nm CW laser diode (2 W) serving as the excitation source. Dynamic light scattering (DLS) was carried out at 298.0 K with a Zetasizer Nano ZS (Malvern) equipped with a solid-state He–Ne laser (λ = 633 nm) for monitoring the variation of the hydrodynamic size of the nanoparticles before and after antibody conjugation. The test strips were excited by the 980 nm fiber laser with a beam size of 2 cm at a distance of 10 cm to completely cover the detection area. Optical images were acquired using a digital camera (EOS450D, Canon), and then processed using ImageJ 1.42q software for analyzing the luminescence signal from the T and C lines.

Results and discussion

Structural analysis of the UCL nanoparticles

TEM was used to characterize the as-prepared $NaGdF_4$:Yb,Er and $NaGdF_4$:Yb,Er@$NaGdF_4$ core–shell nanoparticles. As shown in Fig. 1, the core is rather monodispersed with a spherical particle showing an average size of 15.9 ± 0.6 nm, while the core–shell particles become slightly ellipsoidal in shape exhibiting an average size of 30.5 ± 2.0 × 22.4 ± 1.3 nm. However, the monodispersity remains unchanged, which indicates that no secondary nucleation occurred during the shell coating process. Further, electron diffractometry studies reveal that the shell coating doesn't alter the crystalline structure of the core, *i.e.*, the hexagonal structure, which is favorable for upconversion luminescence. The following ICP-AES measurements reveal the ratios of Gd:Yb:Er in the core and core–shell

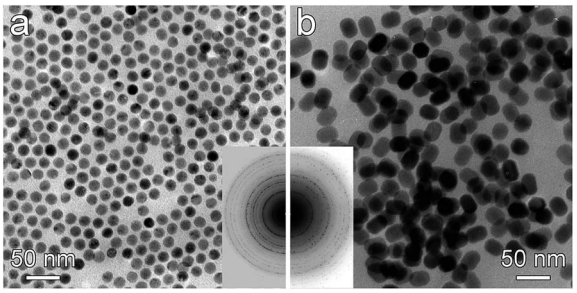

Fig. 1 TEM images of $NaGdF_4$:Yb,Er core particles (a) and $NaGdF_4$:Yb,Er@$NaGdF_4$ core–shell particles (b), insets: electron diffraction patterns of the corresponding nanoparticles.

particles are of 81.1 : 16.6 : 2.3 and 86.7 : 11.7 : 1.6, respectively. These composition data are used for characterising the luminescence enhancement effect in the following section.

Optical properties of UCL core–shell nanoparticles

The UCL spectra of $NaGdF_4$:Yb,Er core and $NaGdF_4$:Yb,Er@$NaGdF_4$ core–shell nanoparticles dispersed in cyclohexane and water are shown in Fig. 2. The major emissions located at 409, 521, 541, and 655 nm can be attributed to radiative relaxations from $^2H_{9/2}$, $^2H_{11/2}$, $^4S_{3/2}$, and $^4F_{9/2}$ states to the $^4I_{15/2}$ state of Er^{3+}, respectively. Compared to core particles dispersed in cyclohexane, the UCL intensity of the major emissions of core–shell ones are all improved due to the shell coating, whereas the integrated UCL is remarkably enhanced by a factor of 136. The luminescence improvement effect provided by the $NaGdF_4$ shell can be explained, according to the literature,[21] as reducing the non-radiative pathways associated with surface defects and depressing the non-radiative emission associated the organic surface ligands bearing alkyl chains. Furthermore, the overall UCL intensity of the $NaGdF_4$:Yb,Er core particles decreases by a factor of 14.2 after being transferred into water through PEGylation. In contrast, the overall luminescence intensity of the core–shell $NaGdF_4$:Yb,Er@$NaGdF_4$ particles only decreases by a factor of 3.3, which suggests that the $NaGdF_4$ shell can significantly help to preserve the luminescence through the phase transfer process. In addition, the core–shell structure is more favorable for maintaining the radiative relaxation from $^2H_{11/2}$ and $^4S_{3/2}$ states to the $^4I_{15/2}$ state of Er^{3+} according to the spectroscopy results. This is highly favorable for the detection sensitivity of LFIA based on UCL particles because the green emissions are very sensitive to naked eyes and Si-based detectors as well.

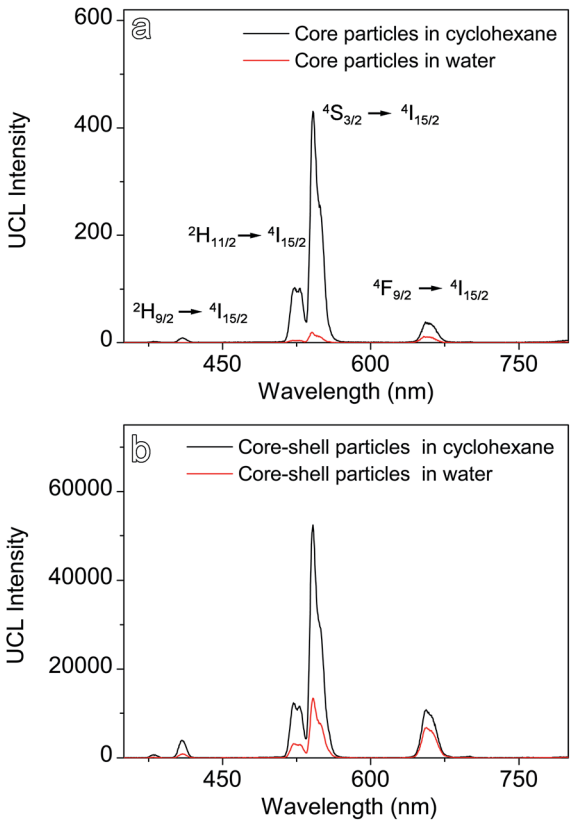

Fig. 2 Normalized luminescence spectra of $NaGdF_4$:Yb,Er core (a) and $NaGdF_4$:Yb,Er@$NaGdF_4$ core–shell nanoparticles (b) dispersed in cyclohexane and water, respectively, recorded upon constant excitation by a CW 980 nm laser.

Conjugate of antibody and UCL nanoparticles

The conjugation reaction between anti-CEX mAb and UCL nanoparticles was investigated by DLS. As shown in Fig. 3, the intensity-weighted mean hydrodynamic size of different samples, denoted as NP and NP–mAb, were 41.1 nm and 61.6 nm, respectively. The reasonable increment in hydrodynamic size and no additional light scattering peaks appeared upon conjugation, indicating that the coupling reaction took place in a controlled manner. After storing for more than 4 months at 4 °C, no precipitation was observed and the hydrodynamic size of conjugate was slightly increased (Fig. S1†). Further spectral results reveal that the upconversion luminescence was almost unchanged after storing for a long time (Fig. S2†).

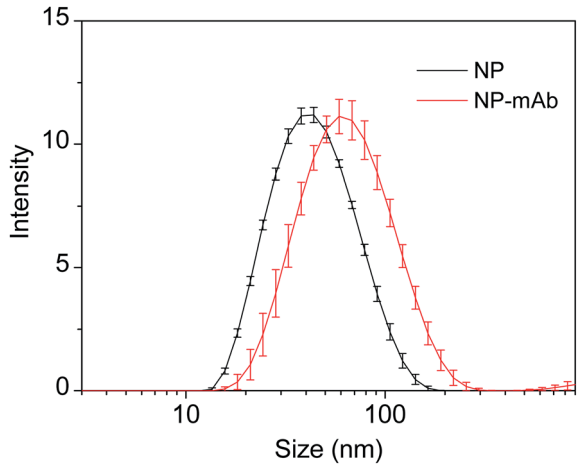

Fig. 3 The hydrodynamic size distribution profiles of the PEGylated core–shell nanoparticles recorded before and after the conjugation reaction with antibody.

UCL nanoparticles-based LFIA for CEX detection

In the following LFIA experiments, the competitive reaction approach is adopted for detecting the model antibiotic CEX. As shown in Scheme 1, when an aqueous solution without CEX is applied onto the sample pad, the NP–mAb conjugates are rehydrated, and consequently released into the migrating liquid, which then migrate across the NC membrane driven by capillary force. Because the immobilized CEX–BSA on the T line can specifically bind with the NP–mAb conjugates, test signal under illumination will be observed at the T line. When CEX is present in the sample solution, it competes with CEX–BSA immobilized on the T line to bind with NP–mAb conjugates. Consequently, the signal of T line becomes inversely proportional to the amount of CEX in the sample, while the C line is functionalized with a secondary antibody and captures the NP–mAb conjugates irrespective of the presence of CEX. However, when C line signal disappears, the test becomes invalid.

Fig. 4 shows the LFIA results based on UCL nanoparticles compared with the colloidal gold nanoparticles-based LFIA results in the CEX detection. Herein, the visual detection limit is defined to be the minimum target analyte concentration required for the T line to show no obvious staining effect. Following this definition, the visual detection limit achieved by both UCL NP–mAb and Au NP–mAb was around 10 ng mL^{-1}, which is below the detection limit that is legislated by the European Union (EU) and Food and Drug Administration (FDA).[17]

To quantitatively extract the detection limit, the luminescence of both the T and C lines were carefully imaged after CEX solutions with gradient concentrations of 0, 0.5, 1, 2, 5, 10, 50, 100, and 500 ng mL^{-1} went across them. Then, the luminescence images were analysed by integrating the cross-section of the T line and C line using Image J. In a similar way, the Au nanoparticles-based LFIA images were analyzed by integrating the optical density of both T line and C line. In both cases, the T line signal was normalized with respect to the C line signal recorded from the same strip. As shown in Fig. 5, the signal intensity of the T line of UCL nanoparticle-labeled and Au nanoparticle-stained LFIA strips significantly decreases against the concentration of CEX. The linear fitting of the dose–response curves reveals that the linear response range is from 0.5 to 100 ng mL^{-1} for both UCL NP–mAb and Au NP–mAb probes, with a correlation coefficient being of 0.9983 and 0.9836, respectively. By defining the detection limit as the minimum concentration of analyte required for inducing a 10% relative optical signal decrease,[22] as guided by the dashed line, it was determined to be 0.3 ng mL^{-1} for Au NP–mAb, and 0.6 ng mL^{-1} for UCL NP–mAb. Although the detection limit remains comparable with colloidal gold nanoparticles-based LFIA, which was achieved under optimized condition according to the previous work,[18] the UCL particles-based LFIA may still be favorable for detecting actual sample due to the low background signal for upconversion luminescence.

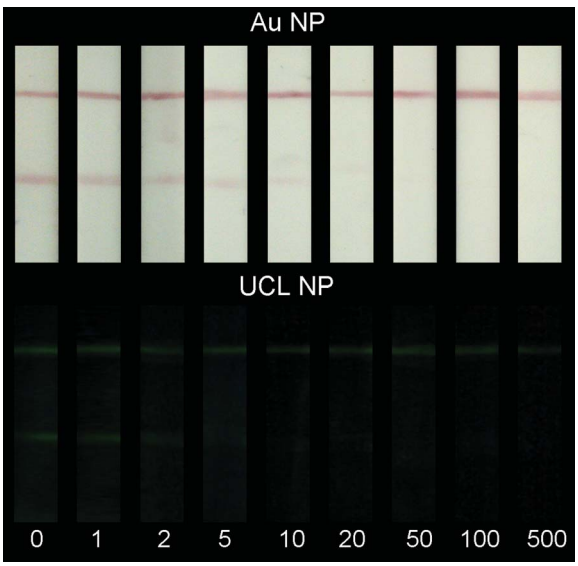

Fig. 4 Photographs for a group of test strips of LFIA based on Au nanoparticles and UCL nanoparticles, respectively, for detecting CEX in different concentrations (ng mL^{-1}) shown below.

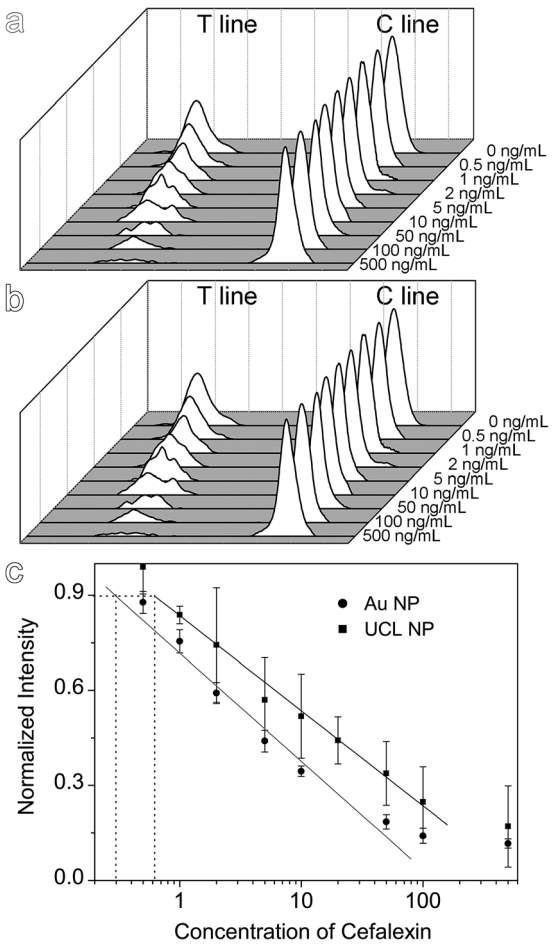

Fig. 5 Optical density profiles of T line and C line recorded using Au NP–mAb (a), luminescence intensity profiles of T line and C line recorded using UCL NP–mAb (b) after applying a series of standard solutions with different CEX concentrations ($N = 4$), and dose–response curves for CEX based on quantitative analysis using Au nanoparticles and UCL nanoparticles, respectively, as antibody labels (c).

Conclusion

A sensitive LFIA method is successfully established for detecting antibiotic CEX through the use of core–shell structured UCL nanoparticles. Because of the $NaGdF_4$ shell coating, the luminescence of the underlying $NaGdF_4$:Yb,Er core is remarkably increased and better preserved through the phase transfer process upon PEGylation, which is beneficial for the high sensitivity of CEX detection. As a result, a visual detection limit of approximately 10 ng mL^{-1} is achieved through upconversion luminescence. Further quantitative analysis reveals that the linear detection range is about 0.5 to 100 ng mL^{-1}, with a sensitivity approaching 0.6 ng mL^{-1}. Based on these investigations, it can be concluded that the UCL nanoparticles-based LFIA becomes an alternative approach for Au nanoparticles-based LFIA, and may become useful for actual sample detection due to low UCL background.

Acknowledgements

The authors thank the NSFC (21203211, 21321063, 21403250, 81471726) and CAS (CMS-PY-201309, CMS-PY-201314).

Notes and references

1 C. Y. Liu, Q. J. Jia, C. H. Yang, R. R. Qiao, L. H. Jing, L. B. Wang, C. L. Xu and M. Y. Gao, *Anal. Chem.*, 2011, **83**, 6778–6784.
2 S. Wang, Y. Quan, N. Lee and I. R. Kennedy, *J. Agric. Food Chem.*, 2006, **54**, 2491–2495.
3 J. Lin and H. Ju, *Biosens. Bioelectron.*, 2005, **20**, 1461–1470.
4 M. Elkjaer, J. Burisch, V. V. Hansen, B. D. Kristensen, J. K. S. Jensen and P. Munkholm, *Aliment. Pharmacol. Ther.*, 2010, **31**, 323–330.
5 P. von Lode, *Clin. Biochem.*, 2005, **38**, 591–606.
6 S. C. Lou, C. Patel, S. F. Ching and J. Gordon, *Clin. Chem.*, 1993, **39**, 619–624.
7 A. Vanamerongen, J. H. Wichers, L. B. J. M. Berendsen, A. J. M. Timmermans, G. D. Keizer, A. W. J. Vandoorn, A. Bantjes and W. M. J. Vangelder, *J. Biotechnol.*, 1993, **30**, 185–195.
8 M. J. Pugia, R. G. Sommer, H. H. Kuo, P. F. Corey, D. L. Gopual and J. A. Lott, *Clin. Chem. Lab. Med.*, 2004, **42**, 340–346.
9 Y. Y. Wang, H. Xu, M. Wei, H. C. Gu, Q. F. Xu and W. Zhu, *Mater. Sci. Eng., C*, 2009, **29**, 714–718.
10 Q. F. Xu, H. Xu, H. C. Gu, J. B. Li, Y. Y. Wang and M. Wei, *Mater. Sci. Eng., C*, 2009, **29**, 702–707.
11 H. Yang, D. Li, R. He, Q. Guo, K. Wang, X. Q. Zhang, P. Huang and D. X. Cui, *Nanoscale Res. Lett.*, 2010, **5**, 875–881.
12 S. Choi, E. Y. Choi, D. J. Kim, J. H. Kim, T. S. Kim and S. W. Oh, *Clin. Chim. Acta*, 2004, **339**, 147–156.
13 Z. H. Li, Y. Wang, J. Wang, Z. W. Tang, J. G. Pounds and Y. H. Lin, *Anal. Chem.*, 2010, **82**, 7008–7014.
14 C. Bouzigues, T. Gacoin and A. Alexandrou, *ACS Nano*, 2011, **5**, 8488–8505.
15 J. Shen, L. D. Sun and C. H. Yan, *Dalton Trans.*, 2008, 5687–5697.
16 W. S. Darwish, E. A. Eldaly, M. T. E-Abbasy, Y. Ikenaka, S. Nakayama and M. Ishizuka, *Jpn. J. Vet. Res.*, 2013, **61**, S13–S22.
17 H. L. Xie, W. Ma, L. Q. Liu, W. Chen, C. F. Peng, C. L. Xu and L. B. Wang, *Anal. Chim. Acta*, 2009, **634**, 129–133.
18 J. Guo, L. Liu, F. Xue, C. Xing, S. Song, H. Kuang and C. Xu, *Food Agric. Immunol.*, 2014, 1–11.
19 Y. Hou, R. R. Qiao, F. Fang, X. X. Wang, C. Y. Dong, K. Liu, C. Y. Liu, Z. F. Liu, H. Lei, F. Wang and M. Y. Gao, *ACS Nano*, 2013, **7**, 330–338.
20 C. Y. Liu, Z. Y. Gao, J. F. Zeng, Y. Hou, F. Fang, Y. L. Li, R. R. Qiao, L. Shen, H. Lei, W. S. Yang and M. Y. Gao, *ACS Nano*, 2013, **7**, 7227–7240.
21 F. Wang, J. A. Wang and X. G. Liu, *Angew. Chem., Int. Ed.*, 2010, **49**, 7456–7460.
22 M. Blazkova, B. Mickova-Holubova, P. Rauch and L. Fukal, *Biosens. Bioelectron.*, 2009, **25**, 753–758.